Mitochondrial DNA Mutations Increase in Early Stage Alzheimer's Disease and are Inconsistent with Oxidative Damage

Jake G. Hoekstra, PhD,[1] Michael J. Hipp, BS, [1] Thomas J. Montine, MD, PhD[2], Scott R. Kennedy, PhD[1*]

Author Affiliation: [1] Department of Pathology, University of Washington, Seattle, WA; [2] Department of Pathology, Stanford University, Palo Alto, CA

Running Head: Mitochondrial mutations in early AD

[*]Corresponding Author
Scott R Kennedy
HSB E506, Box 357470
1959 NE Pacific St
Seattle WA, 98195
Email: scottrk@uw.edu
Phone: (206) 543-5452
Fax: (206) 543-3967

Character Count (Title): 114
Character Count (Running Head): 35
Word Count (Abstract): 99
Word Count (Body): 1502
Figure Count: 2 Main Figures (1 Color; 1 Black/White) and 2 Supplemental (2 Black/White)
Table Count: 1 Main Table and 2 Supplemental Tables

This article has been accepted for publication and undergone full peer review but has not been through the copyediting, typesetting, pagination and proofreading process which may lead to differences between this version and the Version of Record. Please cite this article as an 'Accepted Article', doi: 10.1002/ana.24709

ABSTRACT

Mitochondrial dysfunction and oxidative damage are commonly associated with early stage Alzheimer's disease (AD). The accumulation of somatic mutations in mitochondrial DNA (mtDNA) has been hypothesized to be a driver of these phenotypes, but the detection of increased mutation loads has been difficult due to a lack of sensitive methods. We used an ultra-sensitive next-generation sequencing technique to measure the mutation load of the entire mitochondrial genome. Here, we report a significant increase in the mtDNA mutation frequency in the hippocampus of early-stage AD, with the cause of these mutations being consistent with replication errors and not oxidative damage.

INTRODUCTION

Somatic (non-inherited) mtDNA mutations and mitochondrial dysfunction are thought to be important drivers of aging and age-related neurodegenerative diseases such as Alzheimer's disease (AD) and Parkinson's disease (PD), where mtDNA mutation accumulation may precede the appearance of clinical symptoms.[1] Mutations in mitochondrial DNA (mtDNA), both through inheritance or somatic accumulation, can compromise mitochondrial function and result in cell death and disease.[2, 3] Previous studies investigating the contributions of mtDNA mutations in AD have failed to consistently identify associations between AD and mutations.[4, 5] Such inconsistencies likely stem from three main causes: i) the inclusion of only samples from patients with late stage AD, wherein only the healthiest cells with the lowest mutation loads likely remain; ii) the examination of relatively small regions in mtDNA; and iii) the use of PCR amplification techniques that result in higher error rates due to misincorporation events by DNA polymerase.

To overcome these issues, we examined point mutations and small insertions/deletions across the entire mitochondrial genome purified from the hippocampus and parietal lobe of AD, early stage AD, and healthy control patients using Duplex Sequencing (DS). DS is a highly accurate next-generation sequencing methodology that relies on molecular barcoding and sequencing of both strands of a double-stranded DNA molecule to eliminate both sequencer and PCR derived errors, thus allowing for the detection of a single mutation in $>10^7$ wild-type nucleotides (Fig 1A-C).[6, 7]

MATERIALS AND METHODS

Human Brain Samples

Flash frozen brain tissue was obtained from the Neuropathology Core of the University of Washington Alzheimer's Disease Research Center (Seattle, Washington). All clinical information and consent was obtained according to protocols approved by the University of Washington Institutional Review Board (IRB#24250). Cases were grouped using two criteria: last clinical diagnosis of no dementia (ND, within 2 years of death) or dementia (D) according to criteria from the DSM-IV and pathologic classification for AD by Braak staging[8] ; cases with any other neuropathologic diagnosis, gross infarcts/hemorrhages, Lewy bodies, or ischemic injury were excluded. We stratified cases into three groups: no demenita and Braak none, I, or II (ND/Low-AD); no dementia and Braak III, IV (ND/High-AD); and AD dementia with Braak stage V or VI (D/High-AD) (Table 1, Supplementary Table 1).

Isolation of Synaptosomes and mtDNA from Human Brain Tissue

In an effort to enrich for mtDNA from neurons, we isolated synaptosomes from 100-200 mg of tissue of each case using a previously established protocol.[9] Purity of the resulting synaptosome fraction was evaluated by western blot analysis using antibodies against GFAP (DAKO) and synaptophysin (DAKO) (Fig 1D). DNA was extracted from the synaptosome pellet using the QIAamp DNA Micro kit, following instructions for tissue isolation. The relative purity of each mtDNA prep was determined by qPCR using the following primers sets: Nuclear Primers FR: 5'GGGCACTGATCTACACAGTAAG3' RR: 5'TAGTAAGCGCTCAGCAAAGG3' Mitochondrial Primers FR: 5'CCTCAACAGTTAAATCAACAA3' RR: 5'GCGCTTACTTTGTAGCCTTCA3'

mtDNA Duplex Sequencing and Data Analysis

Duplex tag labeled adapter synthesis and DNA shearing were performed as previously described.[7, 10] Briefly, adapters (Fig 1A) were ligated to sheared DNA using NEBNext Ultra End Repair/dA-Tailing and Ligation modules (New England Biolabs) according to the manufacturer instructions. ~$1x10^6$ copies of adapter ligated mtDNA (determined by qPCR) were PCR amplified using KAPA HiFi DNA polymerase (KAPA Biosystems). The DNA was then used in targeted capture using IDT xGen Lockdown probes (Integrated DNA Technologies) specific for human mtDNA following the manufacturer's instructions. The resulting libraries were sequenced using 101-bp paired-end reads on an Illumina HiSeq 2500.

The raw sequencing data was processed as previously described.[10] A minimum of $1x10^6$ post-processing bases were required for each sample. In order to quantify the frequency of *de novo* events, we used a clonality cutoff excluding any positions with variants occurring at a heteroplasmic level of >1% or a depth of <100X, and scored each type of mutation only once at each genome position (Supplementary Table 2).

Statistics

Statistical significance of mutation frequencies between each disease group and control patients was assessed using an unpaired t-test. To adjust for 3 pairwise comparisons (ND/High-AD vs ND/Low-AD, ND/High-AD vs D/High-AD, and ND/Low-AD vs D/High-AD), Bonferroni correction was applied and significance was set at p=0.017.

RESULTS

Tissue from the hippocampus and parietal lobe were obtained for controls (ND/Low-AD), patients with AD dementia (D/High-AD), and individuals that were not demented, but had high Braak staging characteristic of AD dementia (ND/High-AD) (Supplementary Table 1). This last group does not have neuronal loss and are cognitively normal, but are thought to be at risk of developing AD dementia, thus representing an early stage of AD.[11]

Purification of total DNA from bulk brain tissue indicated a significantly reduced amount of mtDNA in the D/High-AD group relative to both the ND/Low-AD and ND/High-AD groups (Fig 1E), consistent with previous studies showing a reduction in mtDNA amounts in CSF.[12] As AD primarily affects neurons, we next sought to measure the mutation frequency of neuronally derived mtDNA by isolating hippocampal synaptosomes via a percoll step-gradient centrifugation strategy and then assessing the somatic mtDNA mutation frequency using DS. The mutation frequency of mtDNA from ND/Low-AD control hippocampal samples was $1.69\pm0.32x10^{-5}$, in close agreement with previous reports[6], whereas the mutation frequency of ND/High-AD samples exhibited a ~60% increase ($2.77\pm0.35x10^{-5}$, p=0.0009) (Fig 2A). No significant increase was detected in D/High-AD cases, or other brain regions (Fig 2A-B). Small insertion/deletions (<5bp) were slightly increased in the hippocampus of the ND/High-AD group (Figure 2C, p=0.009), but not the D/High-AD group. In assessing differences between the characteristics of the groups, no significant differences were observed between post mortem intervals of any group (Table 1). When considering age, the D/High-AD group was significantly younger than the ND/High-AD group (p=0.017, Student's t-test), and trended lower than the ND/Low-AD controls (p=0.032, Student's t-test). However, age did not significantly correlate with mutation frequency in either the hippocampus (r^2=0.018, df=13, p=0.64, Pearson's correlation) or parietal lobe (r^2=0.053, df=11, p=0.44, Pearson's correlation) indicating that the lower sample age in the D/High-AD samples is unlikely to account for the reduced mutation frequency observed in that sample group.

Oxidative damage to mtDNA has been reported to be increased in several stages related to AD dementia.[13-15] The most frequent DNA alteration produced by oxidative damage is 8-hydroxy-2'-deoxyguanosine, which, when copied past during replication or repair, yields G→T/C→A transversions.[16] Surprisingly, we found no significant increase in this mutation subtype in the hippocampus or the parietal lobe of any sample group (Fig 2E, F), suggesting that regional differences in the brain may not account for our observations. Instead, T→C/A→G and G→A/C→T transitions were the most common mutation subtypes observed in all samples, with these subtypes being increased in the ND/High-AD sample group (Fig 2E, F). These findings are consistent with recent reports showing that transitions and not oxidative damage associated G→T/C→A mutations increase in brain tissue with age.[6, 17]

The occurrence of mutations were dispersed throughout the genome, with a ~3-4-fold elevation in the mutation load in the regulator D-loop (Fig 2D) (positions: 1-576; 16,024-16,569) compared to the coding regions (positions: 577-16,023), consistent with previous work.[6] However, comparison of the relative increase in the mutation frequency of the D-loop vs coding region of the ND/Low-AD and ND/High-AD groups shows no significant change in the distribution of mutations between these two mtDNA regions (Fig 2D), indicating that mutation accumulation does not occur to a different extent in the D-loop compared to the genome's coding region.

DISCUSSION

Utilizing a highly sensitive NGS technique that eliminates sequencing errors associated with PCR and DNA damage, we have measured the mutation frequency of neuronally derived mtDNA from patients with varying stages of AD pathology at sensitivities previously unachievable. Compared to controls, the mtDNA point mutation frequency is significantly elevated in the hippocampus of patients with early stage AD, but not in patients with pathologically confirmed AD dementia, suggesting that mutated mtDNA may be lost as neurons die and the disease progresses. This idea is consistent with our observation that the mtDNA:nDNA ratio is dramatically reduced in our D/High-AD samples (Fig 1E).

Oxidative stress is prevalent in AD and has been hypothesized to be a driving force behind the onset and progression of the disease. Although elevated oxidative damage to mtDNA is a feature of AD and is observed at several stages that precede clinical presentation,[13-15] we did not observe an elevation in G→T/C→A mutations, a canonical signature of oxidative damage to DNA. Instead, we note an increase in transitions, which primarily result from nucleotide deamination or nucleotide misincorporation by DNA polymerase γ during mtDNA replication.[18, 19] Interestingly, deficiencies in replication fidelity, impaired removal of defective mitochondria, and increased mtDNA content have all been reported in AD, suggesting a potential origin for the increase in mtDNA mutation load.[20-22]

Our findings are in contrast to previous studies in early PD and incidental Lewy body disease that report a large increase in G→T/C→A mutations.[23] This striking contrast points to an underlying difference in the etiologies of AD and PD and suggests that, unlike early PD, mitochondrially localized oxidative stress may not be an early contributor to AD. Alternatively, the discordance between our findings and earlier reports could be explained by their use of PCR based assays, which can lead to erroneous misincorporation events, to quantify mutations. Consistent with this possibility is that the mutation frequencies we report here are ~10-fold lower than those reported in these studies,[5, 23] and are in closer agreement with previous studies in humans.[6]

Our data suggest that mtDNA mutations either contribute to the onset of AD or indicate an early change in neuronal mitochondria of AD patients. The similarity of the mutation spectra between the different sample groups suggests a similar mutagenic process, which may represent an "enhanced aging" phenotype in patients with AD pathology. Taken together, our findings may prove useful in the future as a potential biomarker and suggests a potential therapeutic strategy that prevents and/or targets the accumulation of mtDNA mutations in AD.

Acknowledgements

We would like to thank Lawrence Loeb and Alan Herr for their critical review of the manuscript. Support for this research was provided, in part, by the University of Washington Alzheimer's Disease Research Center (NIH P50AG05136). SRK was further supported by the Genetic Approaches to Aging Training Grant (NIA T32-AG000057). The funders had no role in study design, data collection and analysis, decision to publish, or preparation of the manuscript.

Author Contributions

SRK, TJM, and JGH conceived and designed the project. SRK, JGH, MJH collected, analyzed, and interpreted data. SRK and JGH wrote the paper.

Conflicts of Interest

The authors declare no conflicts of interest.

REFERENCES

1. Kennedy SR, Loeb LA, Herr AJ. Somatic mutations in aging, cancer and neurodegeneration. Mech Ageing Dev. 2012 Apr;133(4):118-26.
2. Hayashi J, Ohta S, Kikuchi A, Takemitsu M, Goto Y, Nonaka I. Introduction of disease-related mitochondrial DNA deletions into HeLa cells lacking mitochondrial DNA results in mitochondrial dysfunction. Proc Natl Acad Sci U S A. 1991 Dec;88(23):10614-8.
3. Mashima Y, Saga M, Hiida Y, et al. Quantitative determination of heteroplasmy in Leber's hereditary optic neuropathy by single-strand conformation polymorphism. Invest Ophthalmol Vis Sci. 1995 Jul;36(8):1714-20.
4. Coskun PE, Beal MF, Wallace DC. Alzheimer's brains harbor somatic mtDNA control-region mutations that suppress mitochondrial transcription and replication. Proc Natl Acad Sci U S A. 2004 Jul;101(29):10726-31.
5. Lin MT, Simon DK, Ahn CH, Kim LM, Beal MF. High aggregate burden of somatic mtDNA point mutations in aging and Alzheimer's disease brain. Hum Mol Genet. 2002 Jan;11(2):133-45.
6. Kennedy SR, Salk JJ, Schmitt MW, Loeb LA. Ultra-sensitive sequencing reveals an age-related increase in somatic mitochondrial mutations that are inconsistent with oxidative damage. PLoS Genet. 2013;9(9):e1003794.
7. Schmitt MW, Kennedy SR, Salk JJ, Fox EJ, Hiatt JB, Loeb LA. Detection of ultra-rare mutations by next-generation sequencing. Proc Natl Acad Sci U S A. 2012 Sep;109(36):14508-13.
8. Braak H, Braak E. Neuropathological stageing of Alzheimer-related changes. Acta Neuropathol. 1991;82(4):239-59.
9. Dunkley PR, Jarvie PE, Robinson PJ. A rapid Percoll gradient procedure for preparation of synaptosomes. Nat Protoc. 2008;3(11):1718-28.
10. Kennedy SR, Schmitt MW, Fox EJ, et al. Detecting ultralow-frequency mutations by Duplex Sequencing. Nat Protoc. 2014 Nov;9(11):2586-606.
11. Nelson PT, Braak H, Markesbery WR. Neuropathology and cognitive impairment in Alzheimer disease: a complex but coherent relationship. J Neuropathol Exp Neurol. 2009 Jan;68(1):1-14.
12. Podlesniy P, Figueiro-Silva J, Llado A, et al. Low cerebrospinal fluid concentration of mitochondrial DNA in preclinical Alzheimer disease. Ann Neurol. 2013 Nov;74(5):655-68.
13. Lovell MA, Soman S, Bradley MA. Oxidatively modified nucleic acids in preclinical Alzheimer's disease (PCAD) brain. Mech Ageing Dev. 2011 Aug;132(8-9):443-8.
14. Wang J, Xiong S, Xie C, Markesbery WR, Lovell MA. Increased oxidative damage in nuclear and mitochondrial DNA in Alzheimer's disease. J Neurochem. 2005 May;93(4):953-62.
15. Wang J, Markesbery WR, Lovell MA. Increased oxidative damage in nuclear and mitochondrial DNA in mild cognitive impairment. J Neurochem. 2006 Feb;96(3):825-32.
16. Cheng KC, Cahill DS, Kasai H, Nishimura S, Loeb LA. 8-Hydroxyguanine, an abundant form of oxidative DNA damage, causes G→T and A→C substitutions. J Biol Chem. 1992 Jan;267(1):166-72.
17. Williams SL, Mash DC, Züchner S, Moraes CT. Somatic mtDNA mutation spectra in the aging human putamen. PLoS Genet. 2013;9(12):e1003990.
18. Duncan BK, Miller JH. Mutagenic deamination of cytosine residues in DNA. Nature. 1980 Oct;287(5782):560-1.
19. Zheng W, Khrapko K, Coller HA, Thilly WG, Copeland WC. Origins of human mitochondrial point mutations as DNA polymerase gamma-mediated errors. Mutat Res. 2006 Jul;599(1-2):11-20.
20. Alvarez V, Corao AI, Alonso-Montes C, et al. Mitochondrial transcription factor A (TFAM) gene variation and risk of late-onset Alzheimer's disease. J Alzheimers Dis. 2008 Apr;13(3):275-80.
21. Wang X, Su B, Lee H, et al. Impaired balance of mitochondrial fission and fusion in Alzheimer's disease. J Neurosci. 2009 Jul;29(28):9090-103.

22. Hirai K, Aliev G, Nunomura A, et al. Mitochondrial abnormalities in Alzheimer's disease. J Neurosci. 2001 May;21(9):3017-23.
23. Lin MT, Cantuti-Castelvetri I, Zheng K, et al. Somatic mitochondrial DNA mutations in early Parkinson and incidental Lewy body disease. Ann Neurol. 2012 Jun;71(6):850-4.

Figure 1: Overview of Duplex Sequencing and sample purity. (A) Duplex Sequencing uses a modified form of the Illumina TruSeq adapter design containing a unique complementary random sequence. (B) Ligation of the adapters to sheared DNA (*yellow*) generates unique tags on each end (α and β), such that each molecule has a different tag combination. Reads derived from the Read 1 and Read 2 synthesis reactions of a paired-end run are denoted in purple and green, respectively. (C) PCR amplification of the two strands produces two related, but distinct products. Sequence reads sharing the same α and β combination and the same sequencing reaction (*i.e.* Read 1 or Read 2) are grouped into "families". A consensus sequence for each family is then calculated to form a "single-strand consensus" sequence (SSCS) using a simple majority rules consensus caller. Putative mutations are of three different types: sequencing mistakes or late arising PCR errors (*red* and *purple* spots); first round PCR errors (*brown* spots); and true mutations (*green* spots). Formation of the SSCS removes sequencer mistakes and late arising PCR errors, but is unable to remove first round PCR errors. Comparison of the SSCS with appropriately oriented α and β tags derived from the complementary strands of the original double-stranded DNA generates a double-strand consensus. Figure is adapted from Kennedy *et al.* 2013.[8] (D) Synaptosome fractionation increases the purity of neuronally derived mitochondria. Synaptosomes were purified from crude homogenized brain tissue using a Percoll step gradient fractionation protocol provided by Dunkley *et al*[9]. Only Percoll Fraction 4 was used for sequencing due to a significant enrichment in mtDNA being found in this fraction. Panel includes representative western blots of glial fibrillary acidic protein (GFAP)(*top*) and Synaptophysin (*bottom*), as well as the quantification of the western blots for normal hippocampus. CH=Crude Homogenate, F3=Percoll fraction 3, F4=Percoll fraction 4. (E) Reduced mtDNA content in D/High-AD sample group in both the hippocampus and parietal lobe. Only D/High-AD shows a reduced amount of mtDNA, suggesting that a significant portion of mitochondria are no longer present in advanced dementia. Error bars indicate 1 standard deviation.

Figure 2. Somatic mitochondrial DNA (mtDNA) mutation levels in ND/Low controls, early stage AD (ND/High), and Alzheimer's dementia (D/High). mtDNA was extracted from synaptosomes purified by ultra-centrifugation with a Percoll gradient. The DNA was then sequenced using Duplex Sequencing, as previously described[10]. (A) Overall somatic point mutation frequency in hippocampus. The thick black bars indicate the mean and error bars denote one standard deviation. (B) Overall somatic point mutation frequency in parietal lobe. (C) Overall somatic frequency of insertions and deletions (In/Dels) in the hippocampus. (D) The D-loop harbors ~4X more mutations than the coding regions of the mtDNA, but the ratio is unchanged between the normal and disease states. (E) Mutation spectrum reveals a predominance of T:A→G:C and G:C→A:T transitions that are elevated in ND/High, but not AD. G:C→T:A transversions are in low abundance and are unchanged with respect to disease state. **p*=0.0004, ***p*=0.0002, *ns*=not significant. (F) Mutation spectrum for the parietal lobe reveals that transitions mutations are the predominant mutation type.

Table 1. Sample Characteristics

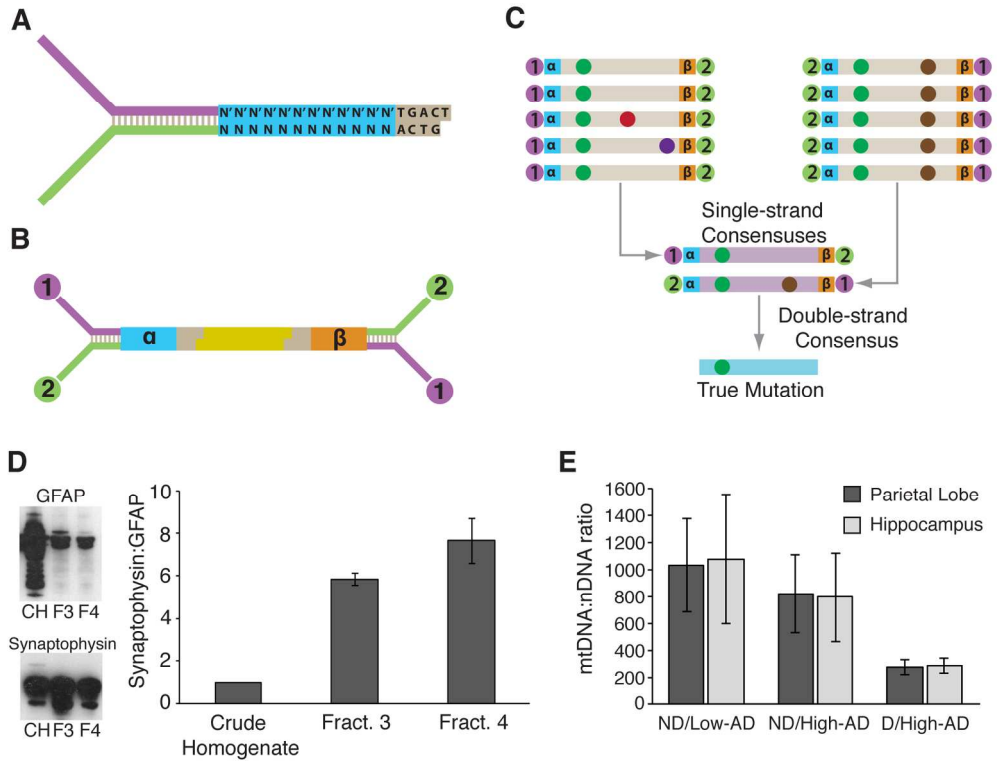

Figure 1: Overview of Duplex Sequencing and sample purity. (A) Duplex Sequencing uses a modified form of the Illumina TruSeq adapter design containing a unique complementary random sequence. (B) Ligation of the adapters to sheared DNA (yellow) generates unique tags on each end (α and β), such that each molecule has a different tag combination. Reads derived from the Read 1 and Read 2 synthesis reactions of a paired-end run are denoted in purple and green, respectively. (C) PCR amplification of the two strands produces two related, but distinct products. Sequence reads sharing the same α and β combination and the same sequencing reaction (i.e. Read 1 or Read 2) are grouped into "families". A consensus sequence for each family is then calculated to form a "single-strand consensus" sequence (SSCS) using a simple majority rules consensus caller. Putative mutations are of three different types: sequencing mistakes or late arising PCR errors (red and purple spots); first round PCR errors (brown spots); and true mutations (green spots). Formation of the SSCS removes sequencer mistakes and late arising PCR errors, but is unable to remove first round PCR errors. Comparison of the SSCS with appropriately oriented α and β tags derived from the complementary strands of the original double-stranded DNA generates a double-strand consensus. Figure is adapted from Kennedy et al. 2013.8 (D) Synaptosome fractionation increases the purity of neuronally derived mitochondria. Synaptosomes were purified from crude homogenized brain tissue using a Percoll step gradient fractionation protocol provided by Dunkley et al9. Only Percoll Fraction 4 was used for sequencing due to a significant enrichment in mtDNA being found in this fraction. Panel includes representative western blots of glial fibrillary acidic protein (GFAP)(top) and Synaptophysin (bottom), as well as the quantification of the western blots for normal hippocampus. CH=Crude Homogenate, F3=Percoll fraction 3, F4=Percoll fraction 4. (E) Reduced mtDNA content in D/High-AD sample group in both the hippocampus and parietal lobe. Only D/High-AD shows a reduced amount of mtDNA, suggesting that a significant portion of mitochondria are no longer present in advanced dementia. Error bars indicate 1 standard deviation.

170x134mm (300 x 300 DPI)

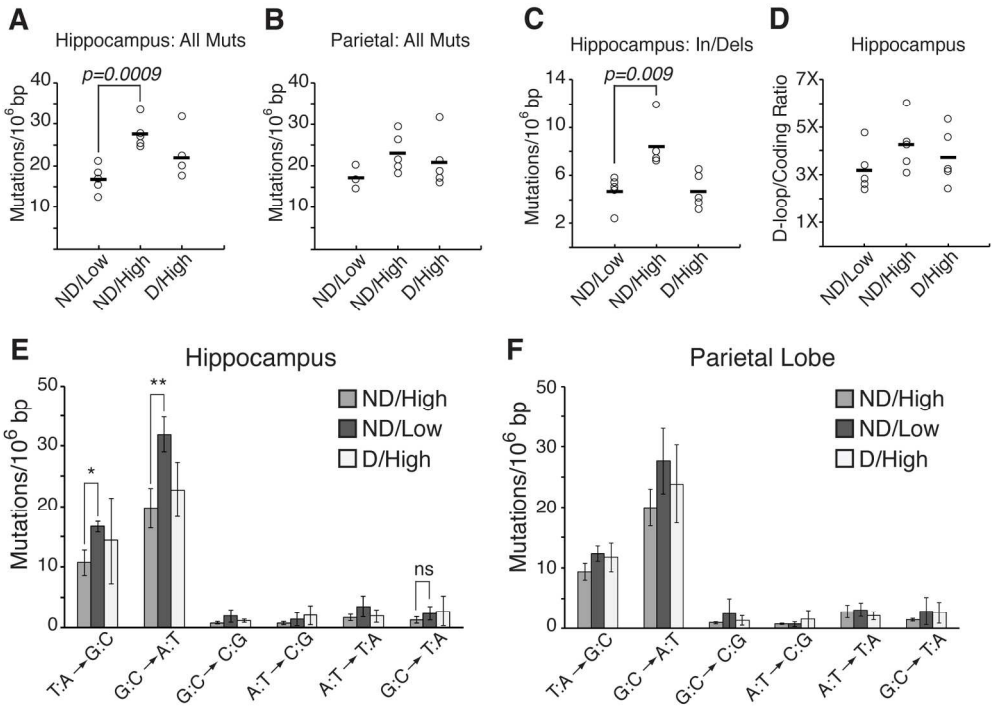

Figure 2. Somatic mitochondrial DNA (mtDNA) mutation levels in ND/Low controls, early stage AD (ND/High), and Alzheimer's dementia (D/High). mtDNA was extracted from synaptosomes purified by ultra-centrifugation with a Percoll gradient. The DNA was then sequenced using Duplex Sequencing, as previously described10. (A) Overall somatic point mutation frequency in hippocampus. The thick black bars indicate the mean and error bars denote one standard deviation. (B) Overall somatic point mutation frequency in parietal lobe. (C) Overall somatic frequency of insertions and deletions (In/Dels) in the hippocampus. (D) The D-loop harbors ~4X more mutations than the coding regions of the mtDNA, but the ratio is unchanged between the normal and disease states. (E) Mutation spectrum reveals a predominance of T:AG:C and G:CA:T transitions that are elevated in ND/High, but not AD. G:CT:A transversions are in low abundance and are unchanged with respect to disease state. *p=0.0004, **p=0.0002, ns=not significant. (F) Mutation spectrum for the parietal lobe reveals that transitions mutations are the predominant mutation type.
169x119mm (300 x 300 DPI)

Table 1. Sample Characteristics

Disease State:	ND/Low	ND/High	D/High
Age yr, mean ± SD	85.8 ± 4.76	88.8 ± 5.76	69.2 ± 13.5
Sex (M/F)	1/4	4/1	2/3
PMI h, mean ± SD	6.03 ± 2.30	4.92 ± 1.59	5.33 ± 1.33
Age of onset yr, mean ± SD	N/A	N/A	60.6 ± 10.64
Disease duration yr, mean ± SD	N/A	N/A	8.6 ± 3.91

ND=No dementia; D= Dementia; PMI= Post-mortem interval; SD=standard deviation

Supplemental Table 1: Sample Details

Case #	Cognitive State/ AD Path.	Region	Age (Years)	Sex	PMI (Hours:Minutes)	Braak Stage	CERAD Score	Disease Duration (Years)
1	ND/Low	H/P	90	M	7:00	II	Sparse	N/A
2	ND/Low	H/P	90	M	5:00	II	Absent	N/A
3	ND/Low	H/P	83	M	8:10	II	Moderate	N/A
4	ND/Low	H	79	F	2:30	II	Absent	N/A
5	ND/Low	H	87	M	7:30	II	Sparse	N/A
6	ND/High	H/P	80	F	4:30	IV	Moderate	N/A
7	ND/High	H/P	92	F	6:00	III	Moderate	N/A
8	ND/High	H/P	86	M	3:00	III	Moderate	N/A
9	ND/High	H/P	94	F	7:00	IV	Frequent	N/A
10	ND/High	H/P	92	F	4:05	IV	Frequent	N/A
11	D/High	H/P	59	F	7:00	VI	Frequent	9
12	D/High	H/P	79	F	4:00	VI	Frequent	8
13	D/High	H/P	59	M	4:00	VI	Frequent	6
14	D/High	H/P	61	M	6:10	VI	Frequent	5
15	D/High	H/P	88	M	5:30	VI	Frequent	15

ND/Low= No Dementia/Low Alzheimer's Pathology; ND/High= No Dementia/High Alzheimer's Pathology; D/High= Dementia/High Alzheimer's Pathology; H=Hippocampus; P=Parietal lobe; M=Male; F=Female; PMI=Post-mortem interval

Supplemental Table 2: Sequencing Details

Case Number	Region	Nucleotides Sequenced	# Point Mutations	A's Sequenced	T'S Sequenced	C's Sequenced	G's Sequenced
1	H	48297000	1018	14809820	11947132	15314930	6225118
	P	16652553	335	5125091	4146004	5227748	2153710
2	H	22544299	383	6956431	5595298	7055591	2936979
	P	22281238	370	6871161	5536966	6984492	2888619
3	H	18367678	338	5611764	4546058	5827721	2382135
	P	45782381	662	14089885	11364313	14483372	5914811
4	H	47887428	743	14785314	11844210	14956243	6301661
5	H	39504707	498	12177647	9793347	12321190	5212523
6	H	8297594	211	2591532	2073969	2569038	1063055
	P	23881491	514	7394820	5910307	7456523	3119841
7	H	6321192	212	2002635	1593864	1951544	773149
	P	1162799	34	405660	322822	298280	136037
8	H	3118531	77	1068804	854728	837454	357545
	P	4028635	80	1301324	1041003	120352	482356
9	H	4878873	132	1557421	1245531	1466035	609886
	P	19305515	350	6177308	4880238	5714999	2532970
10	H	11370869	315	3687485	2947314	3307613	1428457
	P	4037080	106	1250960	1002536	1256904	526680
11	H	26418967	469	8149074	6550984	8289333	3429576
	P	16099193	341	4970471	3987176	5052542	2089004
12	H	2361845	53	732426	592606	732607	304206
	P	4312573	136	1330386	1074091	1347827	560269
13	H	24534673	491	7537899	6094894	7677383	3224497
	P	18815325	321	5811399	4676703	5875624	2451599
14	H	24034868	423	7400983	5943567	7557188	3133130
	P	38116284	608	11653106	9492009	11955466	5015703
15	H	1536287	49	474300	381096	480927	199964
	P	30623401	570	9385773	7610713	9658622	3968293